J. Radiat. Res., 48: Suppl., A15-A25 (2007)

Irradiation System for HIMAC

Masami TORIKOSHI*, Shinichi MINOHARA, Nobuyuki KANEMATSU, Masataka KOMORI, Mitsukata KANAZAWA, Koji NODA, Nobuyuki MIYAHARA, Hiroko ITOH, Masahiro ENDO and Tatsuaki KANAI

HIMAC/Heavy ion therapy/Broad beam method/Wobbler method/Irradiation system/SOBP.

Clinical trials of carbon radiotherapy started at HIMAC in 1994 using three treatment rooms and four beam ports, two horizontal and two vertical. The broad beam method was adopted to make a three-dimensionally uniform field at an isocenter. A spot beam extracted from an accelerator was laterally spread out by using a pair of wobbler magnets and a scatterer. A bar ridge filter modulated the beam energy to obtain the spread out Bragg peak (SOBP). The SOBP was designed to be flat in terms of the biological dose based on the consideration that the field consisted of various beams with different LET. Finally, the field of 20 cm in diameter with ± 2.5% uniformity was formed at the isocenter. The width of the maximum SOBP was 15 cm. When treating the lung or liver, organs that move due to breathing, the beam was irradiated only during the expiration period in a respiration-gated irradiation method. This reduced the treatment margin of the moving target. In order to prevent normal tissues adjacent to the target volume from irradiation by an unwanted dose, a layer-stacking method was developed. In this method, thin SOBP layers which have different ranges were piled up step by step from the distal end to the entrance of the target volume. At the same time, a multi-leaf collimator was used to change the aperture shape to match the shape of each layer to the cross-sectional shape of the target. This method has been applied to rather large volume cancers including bone and soft-tissue cancers. Only a few serious problems in the irradiation systems have been encountered since the beginning of the clinical trials. Overall the systems have been working stably and reliably.

INTRODUCTION

Heavy ion radiation therapy was initiated at Lawrence Berkeley National Laboratory (LBNL), U.S.A using helium ions in 1954 and silicon and neon ions in 1972. More than 450 patients were treated in the clinical trials using neon ion beams[1] before activity was terminated in 1992. In 1990, Loma Linda University Medical Centre started proton radiotherapy for cancers in a hospital based facility. This was the world's first facility equipped with a synchrotron accelerator which was dedicated to clinical applications.[2] The Heavy Ion Medical Accelerator in Chiba (HIMAC) was completed in 1993 as the world's first facility using a heavy-ion accelerator dedicated to medical applications and its clinical trials were started in 1994. Both facilities have been using a broad beam method in which a radiation field was made uniform to cover the target volume using scatterers or a beam wobbling system. A beam scanning method is another way to get a uniform field. A spot-scanning method was developed for proton radiotherapy at the medical cyclotron facility of NIRS in the 1980s.[3] The spot-scanning method has also been employed for proton radiation therapy at Paul Scherrer Institute, Villigen, Switzerland[4] and for heavy ion radiotherapy at Gesellschaft für Schwerionenforschung mbH, Darmstadt, Germany.[5] The spot-scanning method has advantages over the broad beam method as follows: (1) it is possible to generate a large field size without reducing the available beam range, and (2) the number of secondary particles including neutrons is much less than in the broad beam method.

The HIMAC project was started in 1984. At that time, NIRS was carrying out clinical trials of fast neutron radiotherapy and proton radiotherapy using a cyclotron. These clinical experiences were valuable in designing the irradiation system of HIMAC. Development of some apparatuses such as a multi-leaf collimator in which we had no experi-

*Corresponding author: Phone: 043-206-4025,
Fax: 043-251-1840,
E-mail: torikosi@nirs.go.jp
Department of Accelerator and Medical Physics, National Institute of Radiological Sciences, 4-9-1 Anagawa, Inage-ku, Chiba 263-8555 Japan.

ence was started immediately after the project was started. HIMAC started clinical trials in 1994 with three treatment rooms, and a simulation room was additionally constructed on the same floor as the treatment rooms in 1999. Two treatment rooms have a horizontal and vertical beam port each, and one has both horizontal and vertical beam ports. There are two synchrotron accelerators on the first and second floors underground. The latter synchrotron accelerator provides beams with energies of 170, 290 and 400 MeV/n for the horizontal beam ports, and the former provides beams with energies of 140, 290 and 350 MeV/n for the vertical beam ports.

The broad beam method has been well used by a number of facilities doing charged particle radiotherapy; it was especially used and developed for heavy ion radiotherapy at LBNL. Some design concepts of the HIMAC irradiation system were borrowed from those of LBNL. Our expectations have been well realized, and hardly any serious problems have occurred in the last thirteen years. This article briefly introduces the irradiation systems of HIMAC and the irradiation method, including performance and related topics. Biological aspects of the irradiation methods were reported in detail in reference.[6)]

MATERIALS AND METHODS

Use of heavy ion beam in radiation therapy

It is well known that the heavy charged particle beam gives a lower radiation dose at the entrance region but gives a higher dose (Bragg peak) deeper in the medium, furthermore, a high RBE is obtained in the Bragg peak region. These properties of heavy charged particles provide advantageous dose localization for radiotherapy, which can focus on the high dose on a target volume even if it is seated deeply in a body.

Around the beginning of the HIMAC project, there were insufficient data on biological effects of heavy ion beams except for the LBNL data which showed RBE dependence on LET for helium, carbon, neon, silicon and argon. We first excluded helium and argon because helium was considered to have too low an LET and argon was considered to have too high an LET to obtain a good RBE.[8)] Finally, the carbon beam was selected for heavy ion radiotherapy because of the similarity of its LET characteristics to those of the neutron beam which was used for clinical trials at NIRS.[9,10)] The lateral and longitudinal field sizes, the maximum depth, the dose rate and so forth were required from experiences in fast neutron radiotherapy. They were very important to design not only the irradiation system but also the accelerator systems.[11)] Table 1 lists the required field parameters and those in practical use.

Field homogenization and methods

One of key techniques in heavy ion radiotherapy is delivering a prescribed dose to the target volume precisely, accurately and homogeneously. A pristine beam that is extracted from an accelerator has a spot-like beam profile and is mono-energetic. Thus, the beam must be spread out laterally and longitudinally to cover the whole target. In this section, the methods adopted by HIMAC are introduced.

Wobbling beam method

The wobbling beam method is used to laterally spread a spot beam. The spot beam is wobbled by a pair of laminate dipole magnets placed in tandem with their field directions orthogonal to one another. The magnets are sinusoidally excited with an alternating electric current of the same frequency of 56.4 Hz but a 90° phase shift between them. If the amplitudes of the magnetic fields are properly controlled, the spot beam will take a circular track around the original beam axis. When the beam hits a scatterer at the exit of the wobbler magnet, it diverges transversely and draws an annular shape on a plane that is perpendicular to the beam axis. The appropriate combination of the amplitudes of wobbling and the thickness of the scatterer results in a field which has a uniform dose distribution at the isocenter. This method has great advantages over scattering systems in minimizing the

Table 1. Requirement for therapy beams

	Energy (MeV/n)		Range in Water (mm)	Field size (cm)	Field Uniformity	Dose rate (GyE/min)
	Vertical	Horizontal				
Requirements			> 300	ϕ22	< ± 2.5 %	> 5
Practical values	140		38	> ϕ3	< ± 2.5 %	> 10
		170	55			
	290	290	V:155 / H:153	ϕ10		> 5
	350		214	ϕ15		
		400	265	ϕ20		

Note: 140 and 170 MeV/n beams are mainly used for eye treatment.

material in the beam path, while maintaining the beam range. The AC power suppliers are composed of CR resonant circuits to generate a constant frequency. Our wobbling system was developed from experiences in constructing the same type wobbling magnet system at RIKEN ring-cyclotron[12] and at the cyclotron facility in NIRS.[13] The maximum field size produced at the isocenter is 22 cm in diameter. This value satisfies the requirement to treat a 15 × 15 cm^2 target. Homogeneity in the effective area of the field must be ± 2.5% or better. The characteristics of the field such as the lateral dose falloff, and its collimated field size were theoretically analyzed by Tomura *et al.*.[14] They constructed an exact formalism on the basis of a Fermi-Eyges distribution function with consideration of the field divergence by beam wobbling. They derived approximate descriptions from a recurrent calculation of the exact formula by assuming the field uniformity as follows,

$$P_{80\text{–}20} \approx 1.68 \frac{L_W}{L_W - L_C} L_C \sigma_\phi,$$

$$W_{50} \approx \frac{L_W}{L_W - L_C} W_C.$$

$P_{80\text{–}20}$ is the penumbra size that is defined as the width between the 80%–20% dose levels, and W_{50} is the field size defined as the width at the 50% dose level. The parameters L_W, L_C, W_C and σ_ϕ are the distance between the wobbling magnets and the isocenter, the distance between the collimator and the isocenter, the aperture of the collimator and the standard deviation of the angular distribution of beam direction, respectively. Tomura *et al.* compared results obtained with both formalisms with experimental W_{50} and $P_{80\text{–}20}$ values measured at beam energies of 290, 350 and 400 MeV/n for various collimator apertures and various thicknesses of range shifter. Both formalisms gave results that well agreed with the experimental results measured without the range shifter. However, in the region where the range shifter was thick, both gave results that differed by a few percent for W_{50} and about 10% for $P_{80\text{–}20}$. The difference between them was small enough to predict the field properties reasonably well. These formalisms made it possible not only to find parameters of the beam delivery system to minimize the penumbra or maximize the field size but also to optimize parameters of treatment planning.[15]

Energy modulation method

We have adopted bar-ridge filters (RGFs) to modulate the beam energy. When each mono-energetic charged particle penetrates through a different thickness of the bar-ridges, the charged particle loses energy in proportion to the thickness when the incident energy is high. Since the cross-sectional shape of the bar-ridge determines the change of thickness, appropriate design of the bar-ridge enables us to deliver the biological dose to the target region homogeneously. In the case of a heavy ion beam, the SOBP is composed of various LET components with different weighting factors at each depth. The survival rate under mixing LET radiation field was experimentally proved to be described by a formalism proposed in the theory of dual radiation action on the basis of the LQ model.[16] We finally designed the SOBP of mixed charged particles of different LET in accordance with the procedure proposed by Chu *et al.*[1] and the formalism of.[16]

Furthermore, it was also experimentally proven that RBE of HSG cells at around 80 keV/μm in a 6 cm SOBP of a carbon beam with incident energy of 290 MeV/n was equivalent to that of the NIRS fast neutron beam in terms of the biological response.[6] In other words, the neutron-equivalent position in the SOBP was upstream from the distal peak of the SOBP. Experiments also provided information on the dose averaged LET dependence of RBE of HSG cells. Consequently RGFs were designed to make SOBP flat in terms of biological dose with respect to the biological response of HSG cells. The RBE of the neutron-equivalent position in the SOBP was finally normalized to that of the fast neutron radiotherapy as the clinical RBE and was 3.[6]

The RGF is an array of a number of bar-ridges which are interspersed with 5 mm spacing on a plane which is inserted in the beam path. The bar-ridges are made of aluminum or brass; the latter is only for a case of 150 mm wide SOBP. We have 19 kinds of RGFs (Table 2) for SOBP of 2.5 and 30–150 mm. The thinnest RGF is used only for a layer-stacking conformal irradiation described later, and RGFs of

Table 2. RGF width, and thicknesses of RSF and scatterer

No.	RGF: Width (mm)	RSF: Average Thickness (mm)	Scatterer	
			Material	Thickness (mm)
1	2.5	0.30	Ta	0. 105
2	10	0.51	Ta	0. 215
3	15	1.01	Ta	0. 434
4	20*	2.03	Ta	0. 805
5	25*	3.96	Pb	1.6
6	30	7.94	Pb	3.2
7	35	16.06	Pb	6.4
8	40	32.05		
9		64.14		
10	10 mm step	128.11		
~				
16	120			
17	150			

Note:
The RGF with an asterisk indicates there are two types: for normal and for eye specific.

10–25 mm, which were designed for a high dose and low fractions, are used for eye treatments. A typical example of physical dose for SOBP of 400 MeV/n carbon beam measured by a multi-layer ionization chamber (MLIC) is shown in Fig. 1. The field size was 10 cm in diameter, and the SOBP was 6 cm wide. The dots are measured points and the solid line is theoretical values including contribution of fragments.[17] The amplitude of the solid line was calibrated to the dose of the center of the SOBP, and the range was shifted to agree with the distal end of the measured data. Since the theoretical curve was based on the calculated results of the depth dose distribution in water, agreement between the measured data and the calculation was less in the plateau region. The design of RGF is going to be slightly changed to take the contribution of fragments generated in the barridges into consideration.[18]

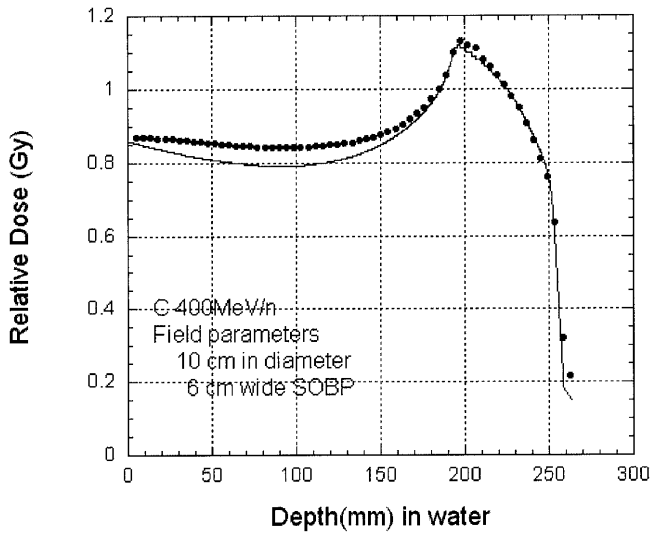

Fig. 1. Depth dose distribution of SOBP of 6 cm width was measured by a multi-layer ionization chamber. The beam energy was 400 MeV/n. The solid line indicates theoretical values. The range and the dose at the center of the SOBP were normalized to the measurement values.

Overview of irradiation systems of HIMAC

There are three treatment rooms and one simulation room about 20 m underground. Treatment rooms A, B and C are equipped with a vertical, vertical and horizontal, and horizontal beam courses, respectively. The configuration of room B is shown in Fig. 2. Both beam ports have the same structure, but the horizontal beam course is slightly longer than the vertical one. Beam transport lines focus the beam on the isocenter without momentum dispersion. The spot beam of about a 1 cm in diameter is provided by the synchrotron accelerator. The wobbler magnets are located 11.7 m upstream from the isocenter of the horizontal beam course and 9.9 m from the isocenter of the vertical beam course. Each magnet has an effective magnetic length of 660.1 mm

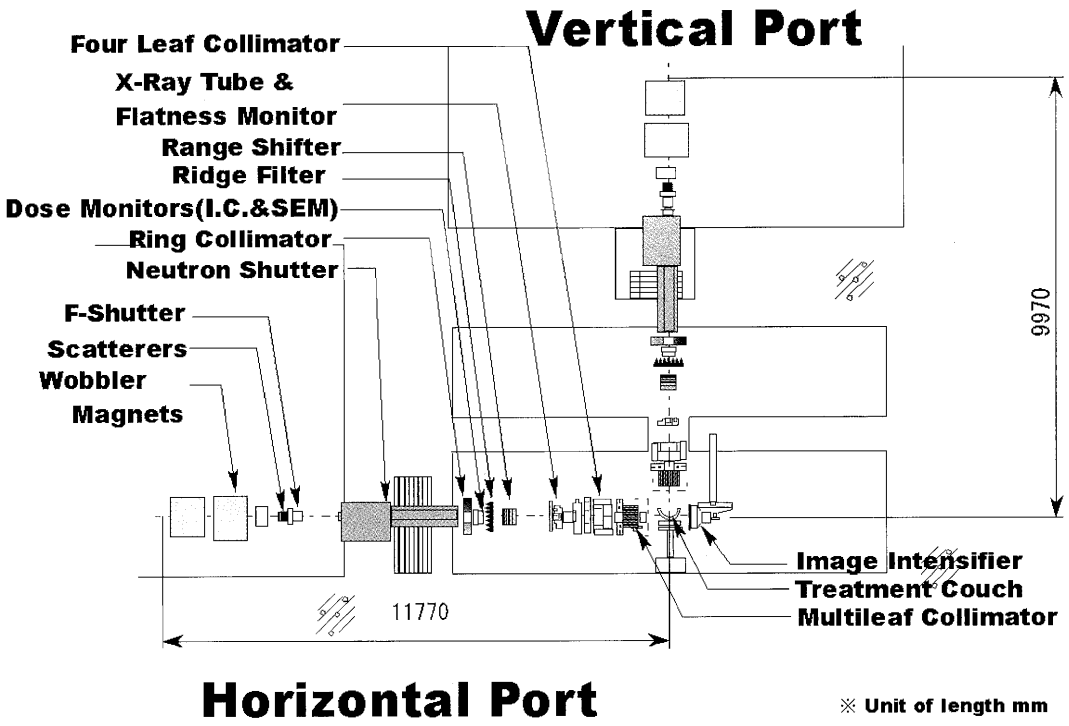

Fig. 2. Beam delivery systems of treatment room B. The horizontal beam port and vertical beam port which have a common isocenter are shown. Both beam ports have the same configuration.

and its pole gap is 110 mm. Both magnets can be excited at 1200 A at the maximum. There is a set of scatterers at the exit of the wobbler magnets. The set contains seven metal sheets which are described in Table 2. Each scatterer is plunged into the beam course by an actuator. The wobbler magnets and scatterers are outside the treatment rooms. Inside the rooms, there are two identical parallel-plate ionization chambers (IC; aperture diameter about 20 cm). They are filled with atmospheric air and operated by applying +2500 V. Each IC consists of three cathodes and two anodes that are staggered with the gap of 5 mm. There used to be other monitors, an ionization chamber and a secondary emission monitor (SEM), to have redundancy by using different type monitors. They were, however, replaced with the present ICs after the high reliability of ICs in practical use was confirmed.[19] One of the ICs works as the main monitor and the other works as the auxiliary monitor. A beam shutter is interlocked to the beam monitors and is closed when the measured dose value reaches the prescribed value. The auxiliary monitor also closes the beam shutter when the measured dose value reaches the value that is larger than the prescribed value by 5%. The RGF system is behind the ICs. Seven RGFs can be set on a disk, and rotating the disk allows selection of any RGF and one empty frame. Fig. 3 shows two RGFs, one made of aluminum and the other made of brass. The laterally enlarged and range-modulated beam is shifted in the range by a constant value with a range shifter (RSF). The RSF consists of ten polymethyl methacrylate (PMMA) plates of various thicknesses as listed in Table 2. Combinations of plates result in thicknesses from 0.25 mm to 255.75 mm in a binary manner. An x-ray tube and a laser light localizer are located about 2.5 m upstream from the isocenter. The laser light localizer has a virtual light source at the middle position of two wobbler magnets to simulate the particle beam. A multi-pad ionization chamber (MPIC) is located about 2 m from the isocenter, which consists of 25 pads of 24 mm in diameter to monitor the lateral uniformity of the field. However, since the field flatness is not satisfied at the location, it is not easy to certify whether the correct field is formed during irradiation. The beam is spatially limited by a four-leaf collimator (FLC) first and a multi-leaf collimator (MLC) second. The MLC consists of 23 pairs of 6.5 mm thick iron plates with 0.25 mm spacing. Fig. 4 shows the MLC used at the horizontal beam port. The leaf with thickness of 140 mm in the beam direction has a tongue-and-groove structure except the central leaf to reduce the inter-leaf dose-leakage. The central leaf has the tongue structure on both sides. The leaf moves at a maximum speed of 80 mm/s and stops at a position with less than $\pm$ 0.5 mm precision. This speed is much faster than that of the MLC used for photon radiotherapy, and this requirement has come from using the layer-stacking irradiation method. The FLC made of aluminum is located just upstream from the MLC. It prevents the MLC from activation due to exposure to the unwanted beam. The FLC also helps the MLC reduce the dose-leakage; the dose-leakage is less than 0.3% when all leaves of the MLC are closed and the FLC is open with an aperture of 5 cm $\times$ 5 cm, and it increases to about 0.6% when the FLC is fully open. The MLC is in use in most treatments excluding the cases of head & neck cancers and brain cancers. In these exceptional cases, finer collimators are used to form the radiation field more precisely. Brass collimators are produced for an individual patient (we call it a *patient collimator*). Patient compensators made of polyethylene are produced for all treatments without exception and are used to conform the distal end of the SOBP to that of the target volume. The number of compensators and/or collimators for a patient depends on the number of portals. The compensator is attached on the end of a nozzle and the patient collimator is attached on it. Since the distance between the end of the nozzle and the isocenter is adjustable between 500 to

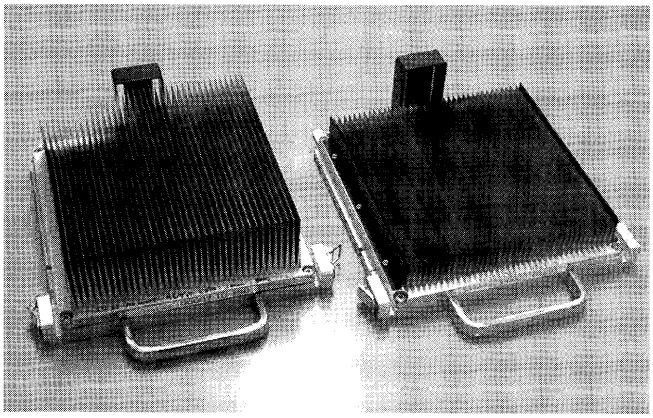

Fig. 3. Ridge filters. The left one is made of aluminum, and the right one of brass.

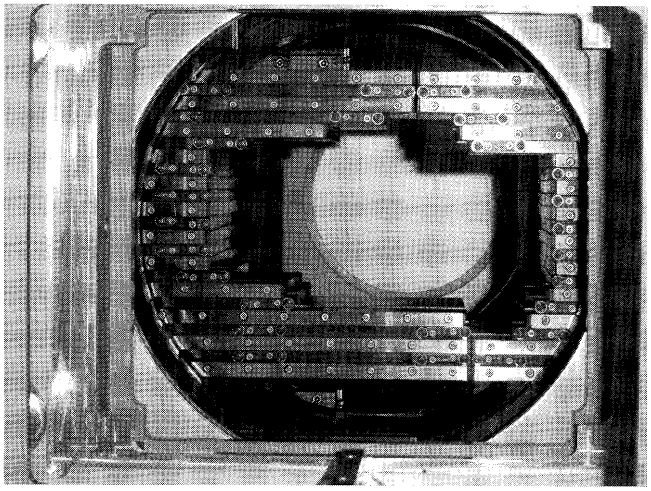

Fig. 4. A multileaf collimator as seen from the downstream side. It has 23 pairs of leaves of 6.5 mm thickness. The maximum aperture is 15 cm $\times$ 22 cm.

Table 3. Distance of each device from isocentre (in unit of meter)

Item	Position	Vertical course In Room A	Horizontal course In Room B
Patient Collimator*	A	0.220	0.224
Patient Compensator*	A	0.348	0.352
Nozzle Head*	A	0.602	0.602
MLC*	A	0.689	0.689
FLC*	A	0.960	0.961
	B	1.170	1.070
Flatness Monitor	A	1.899	2.080
Beam Profile Monitor	C	1.912	2.125
X-Ray Tube	A	1.865	2.275
Light Localizer	A	2.432	2.454
RSF	A	2.254	3.445
	B	2.801	3.898
RGF	A	3.221	4.144
IC(Aux)	C	3.579	4.305
IC(Main)	C	3.703	4.437
Neutron Shutter	A	4.179	4.922
	B	6.911	7.698
F-Shutter	A	6.983	8.544
Scatterer	C	7.443	9.004
Wobbler Magnets	A	7.863	9.606
	B	9.909	11.655
End of HEBT beam duct		10.002	11.803

Note 1: Position indicates the position that was used for measurement of the distance between the device and the isocenter.
A: the nearest point on the device
B: the farthest point on the device
C: the middle between both ends of the device
Note 2: Items with asterisks are moved together. The representative value is indicated by the Nozzle Head distance, which can be changed 0.5–1.0 m from the isocenter.

1000 mm, it is easy to bring the patient collimator into contact with the patient, so that the lateral penumbra is much smaller than when using only the MLC. Distances between each device and the isocenter are listed in Table 3 for the vertical and horizontal beam courses.

We have obtained about 370 parameter sets in which wobbler magnet excitation currents, scatterer thicknesses, RGF heights and RSF thicknesses are included to make uniform fields with various diameters and SOBPs at the isocenter. About 200 sets are in use at treatment planning to choose the most appropriate parameters for an individual treatment.

Irradiation methods

Respiratory-gated irradiation method and system

From the viewpoint of irradiation, organs are divided into roughly two categories: immobile organs such as head & neck and organs moving with a patient's breathing such as lung and liver. For the latter case, the respiration-gated irradiation method is used. The system was developed in 1999 to reduce the treatment margin of the target moving due to breathing.[20] Since then this method has been used for various cases in which there is a fear that the target will move. A patient's chest motion or back motion when the patient

lays prone is detected with an infrared light spot and a position-sensitive CCD camera. In this method, the chest or back motion is assumed to correspond directly to the diaphragm motion. That means that whenever the chest or back returns to the initial position, the target also returns to the initial position. To position a patient, we use digitized fluoroscopic images superimposed on the waveform. The gate signal for beam-on is generated when the phase becomes that of expiration, because the motion of the organ in the expiration phase is slower than that in the inspiration phase and the position of the organ is well reproduced. The beam is extracted from the synchrotron ring using an RF-knockout method within sub-milliseconds after the gate signal becomes logically high.[21] In this method it was proven experimentally that the lateral margin size can be reduced by a factor of 2.0–4.3, depending on the stroke of the motion.[20] However, in some cases, the motion of the organ seems to be more complicated; it was observed that the phase of the respiratory waveform was delayed by about 0.3 s from the phase in which the distance between the entrance (surface) and the target was restored.[22]

Layer-stacking method and system

In the broad beam method, the constant SOBP over the field results in an undesirable dose to the normal tissue proximal to the target.[23] In cancers of the bone and soft tissue seated shallowly with a large volume, 100% of the prescribed dose is sometimes delivered on a skin area in the conventional broad beam method. An improved method for avoiding irradiation of unwanted dose on normal tissue was proposed for proton radiotherapy in 1983[24] and a study was performed in 1996–1998 to examine application feasibility for carbon radiotherapy at HIMAC.[25] In this method, a mini SOBP peak is produced using a short RGF. The RGF is made of aluminum with 2.5 mm height. The full widths at 60% dose level of the peak dose are about 11.9, 12.8 and 15.9 mm for 290, 350 and 400 MeV/n, respectively. In irradiation, the mini peak is longitudinally swept in steps of 2.5 mm with changing thickness of RSF from the distal end of the target volume to the shallowest end, or in the opposite direction.[26] The compensator and MLC are also used as in the ordinary broad beam method, while the shape of the MLC varies as the mini peak moves from one slice to the next.

Through the process of layer-stacking, wobbling amplitudes in x and y directions and the thickness of a scatterer are fixed at the optimized values in spite of inserting various range shifters in the beam course to shift the mini peak. The MLC forms a lateral beam shape to agree with the cross-sectional shape of a certain slice of the target. Once the prescribed dose is delivered on the slice, a preset counter for the main ionization chamber interlocks the beam and gives a trigger signal to move the RSF and MLC and go to the next slice. The beam-on/off control is the same as that for the respiratory-gated irradiation. The interval from one slice to the next is about 100 ms or less. Each leaf of the MLC moves about 80 mm/s at the maximum speed. All parameters (wobbling currents, scatterer index, WEL of RSF, leaf positions of MLC, irradiated dose and so forth) are recorded every slice.

This method is applicable to organs moving due to breathing, by borrowing the technique of the respiratory-gate irradiation. Simulation results showed that the field uniformity depended on the mini peak width and the target motion during the on-gate period.[27] When the target moves only within 2 mm during the irradiation, 100% dose of the prescribed dose is delivered to 95% of the target volume according to DVH. As the mini peak width becomes shorter to reduce hot-spots more, the field uniformity deteriorates more. Besides, as the motion of the target becomes larger, the mini peak width should be larger to keep the field uniformity at a certain level. It is important, therefore, to optimize the overall dose distribution in accordance with the motion of the target.

Positioning and system

The patient lies in a capsule equipped with an immobilization device. The immobilization device consists of fixtures made of polyurethane and shells made of thermoplastic high polymer. The fixtures and shells are made for each patient before CT scanning for treatment planning. The couch for treatment is controlled by six axes (three linear motions and rotations around three axes), but the capsule is used for rolling instead of the couch rolling function because the capsule rotates around the transaxial direction, so that the patient positioning is much easier. When positioning, two radiographic images (a beam's eye view image and its transverse projection image: positioning images) are taken and compared with reference images which were taken in the simulation which is carried out for an individual patient before the first fraction is irradiated. The positioning is basically carried out on using CT images taken during CT scanning for treatment planning. The CT images are reconstructed (digitally reconstructed radiograph image: DRR) and usually used for comparison with the positioning images. However, it takes time to compare the DDR with the positioning images because of the different image quality of DDR from that of the positioning images. Thus, DDR is first used in the simulation for precise positioning, and the reference images are taken for easy comparison with the positioning images.[28] X-ray tubes (125 kV, 400 mA at maximum) are located around 2 m upstream from the isocenter, and a 17-inch image intensifier detector is used to acquire images as a movie. Outlines of the collimator, target and landmarks are superimposed on the positioning image. For the respiratory gated irradiation, the patient's respiratory waveform and the gate signal are also superimposed.[20] The positioning is performed by observing the configuration of the landmarks and fiducial points (mostly bone edges) or that a fiducial point and the other one. Patient positioning takes about 20 minutes

on average.

Dosimetry

In daily operation it is very important to maintain the performance quality of the dose monitoring system. There are three dose monitors for use during the treatment: two parallel plate ionization chambers (ICs) as mentioned in section 2.2 and the MPIC to measure the lateral homogeneity of the beam. The MPIC has an auxiliary parallel plate ionization chamber to bring redundancy into dosimetry. When a beam energy changes, the first two ICs are calibrated by MLIC before treatments start as one of the quality assurance (QA) programs. We call this "*standard dosimetry*" for a certain energy. The MLIC measures the depth-dose distribution (DDD) of the irradiation field that has a lateral size of 10 cm in diameter and 6 cm wide SOBP. The MLIC consists of 64 small cells that are aligned longitudinally. Each cell has a water equivalent length of about 4.5 mm, and forms a parallel plate ionization chamber in which there is a 2 mm gap between an anode and a cathode.[29] The ionization current induced in each cell is integrated and converted to counts. The count is calibrated to the dose at the center of the SOBP measured by the MLIC, and then we obtain a coefficient to convert the IC output [counts] to dose [Gy]. The MLIC is calibrated by a Markus chamber once a year in accordance with the IAEA TRS-398.[30,31] The Markus chamber is also calibrated once a year by a secondary standard chamber in ^{60}Co field. The DDD measurement provides information about the beam range as well as the calibration. Since the beam range depends on the beam energy, ion species, and whether an obstacle is in the beam path or not, the overall QA of the beam is done at the same time.

The irradiation dose at the center of the SOBP changes due to large angle scattered particles when the irradiation field is formed with different parameters.[32] Therefore, for an individual treatment the conversion coefficient [*Gy/count*] is determined with the field parameters specified in the treatment planning for the treatment, we call this "*patient dosimetry*". The patient dosimetry is carried out in the same way as that of the standard dosimetry only once before beginning the treatments. The individual conversion coefficient is determined before the daily treatment by multiplication with the ratio of the average conversion coefficient of standard dosimetry to the daily conversion coefficient of the standard dosimetry which was done on the day when the patient dosimetry was done. Derivation of the individual conversion coefficient from an empirical rule without patient dosimetry is currently being tried.[32]

Control systems

The irradiation systems are classified into functional systems as follows: a man-machine interface system, beam delivery system, dosimetry system, patient positioning system and safety interlock system. Each treatment room has an identical set of control systems consisting of three workstations, one personal computer (PC), and a few PCs to assist in the operation. Another workstation operates as a server computer that interfaces the irradiation control systems with the accelerator control system and the hospital network systems. A number of programmable logic controllers (PLCs) are in use to interface the computers with the devices. These computers and PLCs are connected to each other through a LAN. As mentioned in section 2.3, the dosimetry system directly closes the beam shutter when the measured dose value reaches the prescribed value. The abort-signal generated by not only the dosimetry system but also by any system in which serious problems occur is transmitted to a central interlock system via one of the PLCs through the dual-line of an optical fiber cable and a coaxial metallic cable.[33] This PLC takes the logical OR between all error signals and the dosimetric signal. At the same time, the control system transmits the command to close the beam shutter to the accelerator control system. The central interlock system also commands the beam shutter be closed by software.

RESULTS

A treatment day is initiated by performing the QA program and the standard dosimetry. The standard dosimetry is carried out when changing the beam energy for radiotherapy. The standard dosimetry is usually followed by a few cases of the patient dosimetry. The standard dosimetry provides not only the conversion coefficient but also the daily performance of the dosimetry system. We check that the daily conversion coefficient does not deviate more than ± 1% from the average of the past days, and we judge whether the system works well or not. Fig. 5 shows the variation in the daily

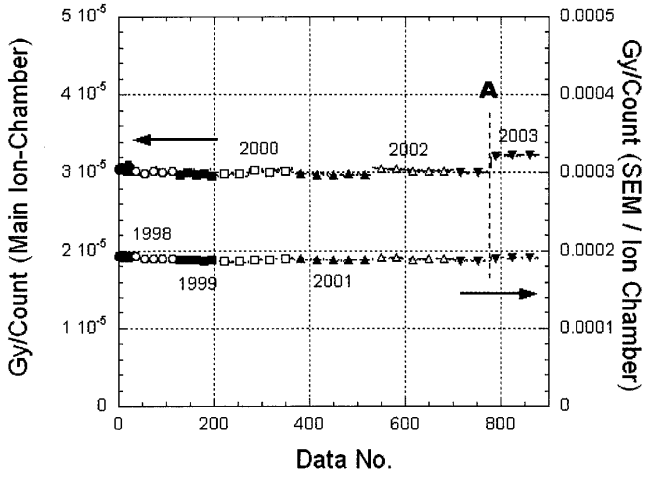

Fig. 5. The ratio of the dose of SOBP center measured by MLIC to the dose measured by the main monitor (ion-chamber) and the sub-monitor (SEM/ion-chamber). Data were accumulated from 1997 to 2002 and for a part of 2003.

conversion coefficient for the past four years of Room A. There is a fluctuation of about ± 1% or less within each year, but considerable change appears one or two times a year because of calibration of the MLIC or replacement of ionization chambers.

Typically, therapy begins at around 9:30 in the morning. Positioning takes about 15–20 minutes, and irradiation takes less than 1 minute for normal irradiation and 1–2 minutes for the respiration-gated irradiation. This positioning time is for a good case. Sometimes it takes about an hour if the markers embedded in the patient's body to be used for positioning have moved or the patient has a bad condition such as strong pain.

The respiration-gated irradiation method is applied to about a half of all treatments. Although a stable waveform is desirable in this method, we have frequently experienced a gradual decrease in the waveform amplitude. This may be because the infrared light source which is taped on the patient's skin has become loosened or sometimes the patient has fallen asleep. The former case may require readjustment of the light source and the camera.

Clinical use of the layer-stacking irradiation method was started in 2003 after a long commissioning period.[34] It has been applied to only nine cases in which targets were static. Four cases were bone and soft-tissue cancers and one was rectum cancer; all of these had large volumes and were located near surfaces. The main concern in these cases was to protect skin from unwanted irradiation. Irradiation is done for 20–40 slices at the rate of about two slices per one beam spill; one spill lasts about 1.5 s. The treatment time is about three or four times more than that of the normal irradiation. The rate of two slices per one beam spill is the maximum speed of performance in order to guarantee precise and reliable operation of the devices. In November 2005 some problems were found in the irradiation system which might prevent safe use of this method. This method also puts heavy loads on the MLCs and RSFs as well. At present, service has been interrupted to upgrade the irradiation system and to improve the MLCs to allow quick and many motions in one treatment.

Patient compensators are indispensable for all treatments, while patient collimators are required for only about 30% of all treatments. Both compensators and collimators are manufactured in a machine shop of NIRS and by an outside company. In a week, about 50–70 compensators and 10–20 collimators are newly used in the treatment rooms.

The number of daily treatments has been increasing year by year. Recently, around 60 treatments are being carried out everyday, so that the treatments end at 19:00–20:00. Therefore, once even a minor problem occurs, it can lead to a big delay in the end time. So far, all the irradiation systems have been running stably and reliably. However, we experienced serious problems a few times in the past that brought about cancellation of some of the treatments scheduled on the day. Most problems were solved within the day by repair work or taking temporary measures. When a treatment room is closed due to some problem, the scheduled treatments can be transferred to the other rooms. All treatment rooms are in principle compatible in terms of field conditions and operation. Software for controlling the irradiation systems has had latent problems since beginning operation because it has been growing complicated due to regular version upgrades for adding optional functions. It should be notable that aging of the devices and the system can not be ignored.

Activities for research and development

We are carrying out a number of research and development activities. The following are some examples. As one of the preparations for aging of the devices, etc., we have been developing a new MLC that has a thinner leaf than the present one. The design concept we are following keeps most specifications of the present MLC, but some have been reconsidered and revised from experiences of the past treatments: considerations have been given to slowing down the leaf speed, simplification of the leaf structure, thinning the leaf thickness, widening the aperture and so forth. A prototype was completed in 2006 and since then various tests are being carried out. The thin leaf MLC is expected to reduce the number of patient collimators needed.

Secondary radioactive beams such as ^{11}C are useful for visualizing the irradiated area. This technique is under development at a secondary beam line of HIMAC.[35] It was experimentally proved that it was possible to determine the end of the ^{11}C range with a precision of less than 1 mm using a positron camera. The final goal is to correct the treatment planning for a patient using the information on the actual dose distribution in the patient's body.

An electron density is indispensable to calculate the range of the heavy ion in treatment planning. Since the electron density is derived from the CT-number acquired by CT scanning, it is thought to have a few percent error due to uncertainty of the CT-number. Heavy ion CT[36,37] and dual-energy x-ray CT can directly provide the electron density. It was experimentally proved that the electron density was measured as accurately as ± 1% or less in the dual-energy x-ray CT.[38]

A spiral wobbler method to make the broad beam has been developed as one of our missions in which we have been working to downsize facilities for heavy ion radiotherapy. This technique can shorten the beam delivery line, and can promote highly efficient use of the beam. In this method, modulation of the amplitude for wobbling the beam draws a spiral trajectory or any other trajectory shape instead of a circular trajectory with a constant diameter at the isocenter. In this method, the beam is less scattered than in the normal wobbler method. This method was successfully used to form fields with uniformity of 3–4%. However, it takes time to make the field with a certain level of uniformity as predicted in the simulation. This must be investigated if the method is applied to moving targets.

Other developments and improvements of the irradiation system, dosimetry and its detectors, etc. are being carried out. Of note among them, we began a new project for development of the next generation irradiation method in 2006. Our goal is the performance of radiotherapy of moving organs by the beam scanning method. Now the respiratory-gated method is under consideration for moving targets. There is the common problem with the case of the spiral wobbler method.

SUMMARY

The irradiation system of HIMAC has been working reliably and stably since the beginning of clinical trials in 1994. There have been improvements, upgrades and developments such as the introduction of the respiration-gated irradiation method and the layer-stacking irradiation method as irradiation methods and use of new detectors such as the MLIC. The number of treatments has been increasing year by year. At the same time, loads on the devices have become heavier, so superannuation of the devices or the systems may become serious someday. Careful maintenance and QA efforts are becoming increasingly important for maintaining high level reliability and safety.

REFERENCES

1. Chu, W. T., Ludewigt, B. A. and Renner, T. R. (1993) Instrumentation for treatment of cancer using proton and light-ion beams. Rev. Sci. Instrum. **64**: 2055–2122.
2. Coutrakon, G., Hubbard, J., Johanning, J., Maudsley, G., Slaton, T. and Morton, P. Performance study of the Loma Linda proton medical accelerator. Med. Phys. **21**: 1691–1701.
3. Kanai, T., Kawachi, K., Kumamoto, Y., Ogawa, H., Yamada, T. and Matsuzawa, H. (1980) Spot scanning system for proton radiotherapy. Med. Phys. **7**: 365–369.
4. Pedroni, E., Bacher, R., Blattmann, H., Boehringer, T., Coray, A., Lomax, A., Lin, S., Munkel, G., Scheib, S., Schneider, U. and Tourovsky, A. (1995) The 200-MeV proton therapy project at the Paul Scherrer Institute: Conceptual design and practical realization. Med. Phys. **22**: 37–53.
5. Haberer, T., Becher, W., Schard, D. and Kraft, G. (1993) Magnetic scanning system for heavy ion therapy. Nucl. Instrum. Methods **A330**: 296–305.
6. Kanai, T., Endo, M., Minohara, S., Miyahara, N., Koyama-Itoh, H., Tomura, H., Matsufuji, N., Futami, Y., Fukumura, A., Hiraoka, T., Furusawa, Y., Ando, K., Suzuki, M., Soga, F. and Kawachi, K. (1999) Biophysical characteristics of HIMAC clinical irradiation system for heavy-ion radiation therapy. Int. J. Radiat. Oncol. Biol. Phys. **44**: 201–210.
7. Bragg, W. H. and Kleeman, R. (1904) On the ionization curves of radium. Phil. Mag. **8**: 726–738.
8. Yamada, S., Takada, E., Kohno, T. and Noda, K. Construction, Commissioning and Pre-clinical Studies of Heavy Ion Medical Accelerator in Chiba (HIMAC). (1995) In: HIMAC report. NIRS Publication NIRS-M-109:HIMAC-009.
9. Morita, S., Arai, T., Nakano, T., Ishikawa, T., Tsunemoto, H., Fukuhisa, K. and Kasamatsu, T. (1985) Clinical experience of fast neutron therapy for carcinoma of the uterine cervix. Int. J. Radiat. Oncol. Biol. Phys. **11**: 1439–1445.
10. Mizoe, J. E., Aoki, Y., Morita, S. and Tsunemoto, H. (1993) Fast neutron therapy for malignant gliomas – results from NIRS study. Strahlentherapie und Onkologie **169**: 222–227.
11. Sato, K., Yamada, S., Ogawa, H., Kawachi, K., Araki, N., Itano, A., Kanazawa, M., Kitagawa, A., Kohno, T., Kumada, M., Murakami, T., Muramatsu, M., Noda, K., Sato, S., Sato, Y., Takada, E., Tanaka, A., Tashiro, K., Torikoshi, M., Yoshizawa, J., Endo, M., Furusawa, Y., Kanai, T., Koyama-Ito, H., Matsufuji, N., Minohara, S., Miyahara, N., Soga, F., Suzuki, M., Tomura, H. and Hirao, Y. (1995) Performance of HIMAC, Nucl. Phys. **A588**: c229–c234.
12. Ohara, H., Kanai, T., Ando, K., Kasai, K., Isukaichi, H., Fukutsu, K., Kawachi, K. and Sato, K. (1991) Accelerator plan for medical treatment with charged particles at Kyoto University. In: Proc. of the NIRS Int. Workshop of Heavy Charged Particle Therapy and Related Subjects. . Eds. Itano, A. and Kanai, T. pp.13–22. Chiba.
13. Kanai, T., Kawachi, K. and Hiraoka, T. (1991) An irradiation facility and a beam simulation program for proton radiation therapy, Nucl. Instrum. Methods. **A302**: 158–164.
14. Tomura, H., Kanai,T., Higashi, A., Futami, Y., Matsufuji, N., Endo, M., Soga, F. and Kawachi, K. (1998) Analysis of the penumbra for uniform irradiation fields delivered by a wobbler method. Jpn. J. Med. Phys. **18**: 42–56.
15. Endo, M., Koyama-Ito, H., Minohara, S., Miyahara, N., Tomura, H., Kanai, T., Kawachi, K., Tsujii, H. and Morita, K. (1996) HIPLAN – A heavy ion treatment planning system at HIMAC. J. Jpn. Soc. Ther. Radiol. Oncol. **8**: 231–238.
16. Kanai, T., Furusawa, Y., Fukutsu, K., Itsukaichi, H., Eguchi-Kasai, K. and Ohara, H. (1997) Irradiation of mixed beam and designing of spread-out Bragg peak for heavy-ion radiotherapy Radiat. Res. **147**: 78–85.
17. Sihver, L., Tsao, C.H., Silberberg, R., Barghouty, A. F. and Kanai, T. (1995) Calculation of depth-dose distributions, cross sections and momentum loss. Adv. Space. Res. **17**: 105–108.
18. Komori, M., Kanai, T., Kanematsu, N., Takei, Y., Yonai, S. and Koikegami, (2006) H., Design of ridge filter for carbon ion radiotherapy Jpn. J. Med. Phys. **26**: 127–128 (in Japanese).
19. Kanai, T., Sudo, M., Matsufuji, N. and Futami, Y. (1998) Initial recombination in a parallel-plate ionization chamber exposed to heavy ions, Phys. Med. Biol. **43**: 3549–3558.
20. Minohara, S., Kanai, T., Endo, M., Noda, K. and Kanazawa, M. (2000) Respiratory gated irradiation system for heavy-ion radiotherapy. Int. J. Radiat. Oncol. Biol. Phys. **47**: 1097–1103.
21. Noda, K., Kanazawa, M., Itano, A., Takada, E., Torikoshi, M., Araki, N., Yoshizawa, J., Sato, K., Yamada, S., Ogawa, H., Itoh, H., Noda, A., Tomizawa, M. and Yoshizawa, M. (1996) Slow beam extraction by a transverse RF field with AM and FM. Nucl Instrum Meth. **A 374**: 269–277.
22. Minohara, S., Endo, M., Kanai, T., Kato, H. and Tsujii, H. (2003) Estimating uncertainties of the geometrical range of particle radiotherapy during respiration, Int. J. Radiat. Oncol. Biol. Phys. **56**: 121–125.

23. Kanematsu, N., Endo, M., Futami, Y., Kanai, T., Asakura, H., Oka, H. and Yusa, K. (2002) Treatment planning for the layer-stacking irradiation system for three-dimensional conformal heavy-ion radiotherapy. Med Phys. **29**: 2823–2829.
24. Kanai, T., Kawachi, K., Matsuzawa, H. and Inada, T. (1983) Broad beam three-dimensional irradiation for proton radiotherapy. Med. Phys. **10**: 344–346.
25. Futami, Y., Kanai, T., Fujita, M., Tomura, H., Higashi, A., Matsufuji, N., Miyahara, N., Endo, M. and Kawachi, K. (1999) Broad-beam three-dimensional irradiation system for heavy-ion radiotherapy at HIMAC, Nucl. Instrum. Method. **A430**: 143–153.
26. Schaffner, B., Kanai, T., Futami, Y., Shimbo, M. and Urakabe, E. (2000) Gidre filter design and optimization for the broad-beam three-dimensional irradiation system for heavy-ion radiotherapy. Med. Phys. **27**: 716–724.
27. Komori, M., Kanematsu, N., Minohara, S. and Kanai, T. (2004) Effect of respiratory motion on dose uniformity with layer-stacking irradiation system. Jpn. J. Med. Phys. **24**: 105–106 (in Japanese).
28. Minohara, S. (1998) Current status of patient positioning at HIMAC. Radioisotopes **47**: 29–37 (in Japanese).
29. Shimbo, M., Urakabe, E., Futami, Y., Yusa, K., Yamashita,, H., Matsufuji, N., Akagi, T., Higashi, A. and Kanai, T.(2000) Development of a multi-layer ion chamber for measurement of depth dose distributions of heavy-ion therapeutic beam for individual patients. Nippon Acta Radiologica **60**: 274–279 (in Japanese).
30. Kanai, T. (2000) Heavy-ion radiotherapy In: Proc. of Atomic and Molecular Data and Their Applications. Eds. Berrington, K. A. and Bell, K. L. pp.25–35.
31. IAEA, Absorbed dose determination in external beam radiotherapy (2000) In: Technical Report Series 398, IAEA, Vienna.
32. Kusano, Y., Kanai, T., Kase, Y., Matsufuji, N., Komori, M., Kanematsu, N., Ito, A. and Uchida, H. (2007) Dose contributions from large-angle scattered particles in therapeutic carbon beams. Med. Phys. **34**: 193–198.
33. Katsumata, M., Kai, S., Kondo, T., Ogawa, H., Kohno, T., Takada, E., Torikoshi, M. and Yamada, S., Beam interlock system for medical accelerator complex HIMAC, Proc. The 13th Symp. on Accel. Sci. and Tech., Suita, Osaka, Japan, Oct. 2001, 408–410.
34. Kanai, T., Kanematsu, N., Minohara, S., Komori, M., Torikoshi, M., Asakura, H. Ikeda, N., Uno, T. and Takei, Y. (2006) Commissioning of a conformal irradiation system for heavy-ion radiotherapy using a layer-stacking method. Med Phys. **33**: 2989–2997.
35. Torikoshi, M., Kanazawa, M., Kouda, S., Kitagawa, A., Murakami, T., Noda, K., Sato, Y., Takada, E., Yoshizawa, J., Futami, Y., Higashi, A., Kanai, T., Matsufuji, N., Tomura, H., Yamada, S., Ishikawa, Y., Tsubuku, H. and Kato, T. (1996) Secondary beam course in HIMAC for applications of medicine and nuclear physics. In: Proc. of Int. Symp. on Non-Nucleonic Deg. Of Freedom Detected in Nuclei. Eds. Minamisono, T. Nojiri, Y., Sato, T., Matsuta, K. pp.401–404 Osaka.
36. Ohno, Y., Kohno, T., Matsufuji, N. and Kanai, T. (2004) Measurement of electron density distribution using heavy ion CT. Nucl. Instrum. Meth. **A 525**: 279–283.
37. Shinoda, H., Kanai, T. and Kohno, T. (2006) Application of heavy-ion CT. Phys. Med. Biol. **51**: 4073–4081.
38. Torikoshi, M., Tsunoo, T., Sasaki, M., Endo, M., Noda, Y., Ohno, Y., Kohno, T., Hyodo, K., Uesugi, K. and Yagi, N. (2003) Electron density measurement with dual-energy x-ray CT using synchrotron radiation. Phys. Med. Biol. **48**: 673–685.

Received on February 13, 2007
1st Revision received on March 12, 2007
2nd Revision received on March 23, 2007
Accepted on March 23, 2007